Supplement of Atmos. Chem. Phys., 19, 1649–1664, 2019
https://doi.org/10.5194/acp-19-1649-2019-supplement

Atmospheric Chemistry and Physics
Open Access
EGU

Supplement of

Physical properties of secondary photochemical aerosol from OH oxidation of a cyclic siloxane

Nathan J. Janechek et al.

Correspondence to: Charles O. Stanier (charles-stanier@uiowa.edu)

Table of Contents

Section S1: General information 1
Table S1 1
Figure S1 2
Figure S2 2
Section S2: D_5 gas sampling quality control results 3
Section S3: D_5 gas sampling details 3
Table S2 3
Figure S3 4
Table S3 5
Figure S4 6
Section S4: Particle loss correction 7
Figure S5 7
Figure S6 8
Table S4 8
Figure S7 9
Section S5: Yield sensitivity 14
Figure S8 14
Section S6: Condensational sink input 15
Table S5 15
Section S7: Hygroscopicity 16
Figure S9 16
Figure S10 16
Figure S11 18
Figure S12 20
Table S6 21
Section S8: Volatility 22
Table S7 22
Figure S13 23
Figure S14 24
References 25

Section S1: General information

Table S1: Experiments performed, chamber settings, and analysis methods for the generation and characterization of cVMS secondary aerosol.

Flow (LPM)	Ring Flow (LPM)	RH (%)	Water Bath (°C)	Lights (%)	Purpose	Analysis	Notes
3.5	1	45	70	80	Yield 1	SMPS, D_5 gas, SO_2 gas	SMPS far
3.5	1	25	60	80	Yield 2	SMPS, D_5 gas, SO_2 gas	SMPS near
5	3	25	70	80	Yield 3	SMPS, D_5 gas, SO_2 gas	SMPS far
3.5	1	45	60	100	Yield 4	SMPS, D_5 gas, SO_2 gas	SMPS far
5	3	25	60	100	Yield 5	SMPS, D_5 gas, SO_2 gas	SMPS near
3.5	1	25	50	80	Seed test	SMPS	
3.5	1	25	60	off	QC test - D_5 chamber test to verify photochemical reaction the source of D_5 loss	SMPS, D_5 gas	
3.5	1	25	70	off	QC test - SPE cartridge breakthrough	D_5 gas	Tested upstream only
-	-	-	-	-	Ammonium sulfate CCN calibration	DMT-CCN, CPC	
5	3	30	70	100	cVMS CCN measurement	DMT-CCN, CPC	
5	3	30	-	100	Antiperspirant oxidation test 1	SMPS	
5	3	30	-	100	Antiperspirant oxidation test 2	SMPS, TPS100	
5	3	30	-	100	Hair conditioner oxidation test 1	SMPS	
5	3	30	70	100	Volatility measurement	SMPS, V-TDMA	
-	-	-	-	-	Heating of D_5 vapor to 100 - 250°C	SMPS	
-	-	-	-	-	Heating of D_5 vapor to 550°C	SMPS	
-	-	-	-	-	Heating of D_5 vapor to 550°C and 80 nm ammonium sulfate seed aerosols	SMPS	

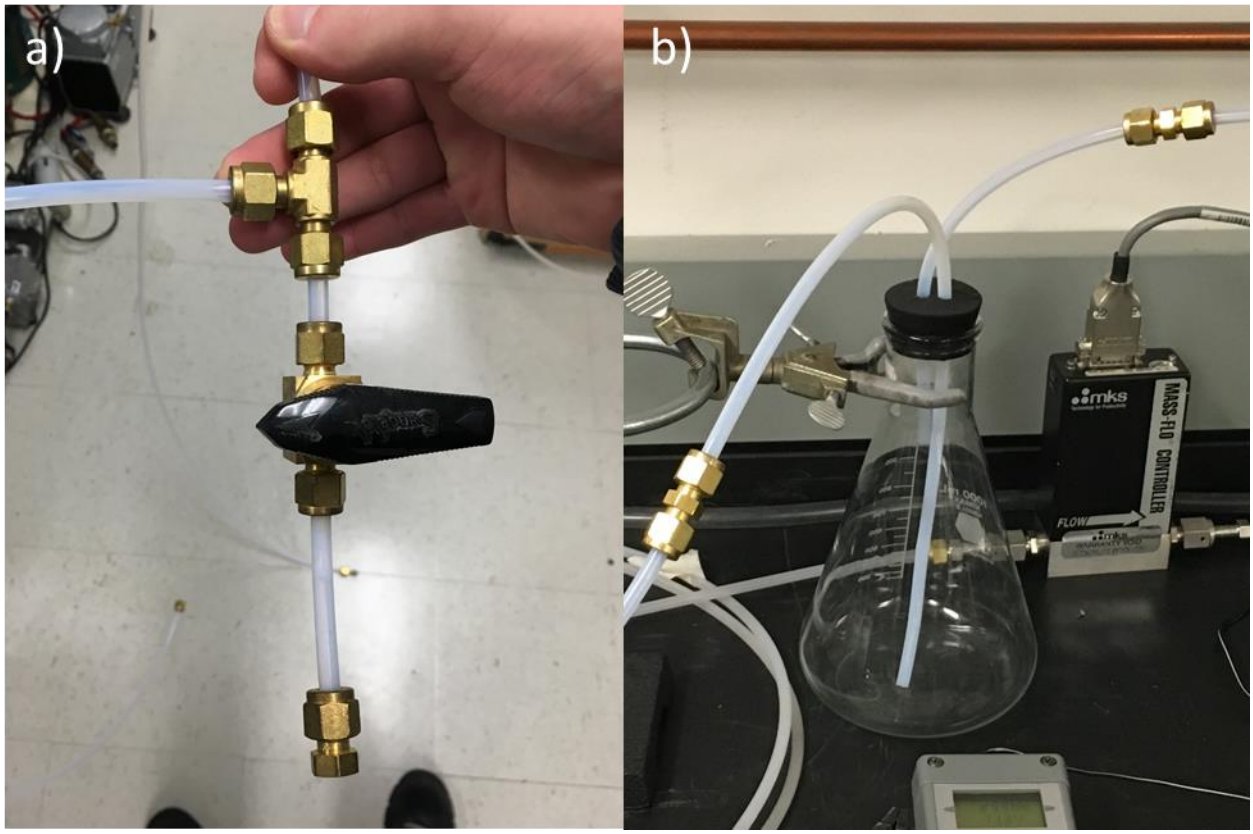

Figure S1: Cyclic siloxane delivery for a) liquid D_5 diffusion and b) flowing air past personal care product.

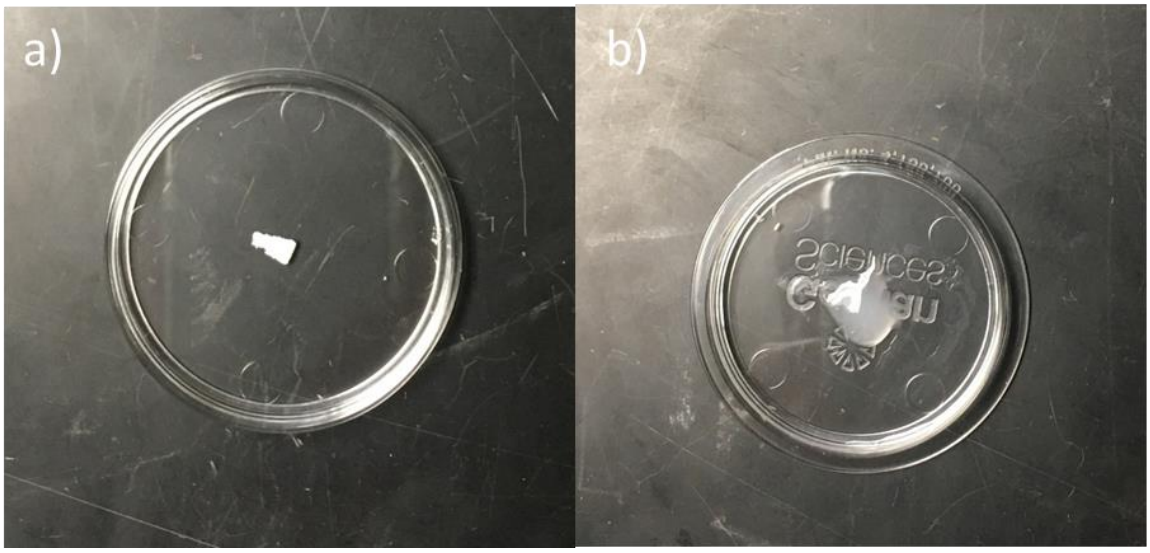

Figure S2: Representative amounts of personal care product placed in flask for cyclic siloxane delivery. Panel a) ~10 mg antiperspirant, and b) ~25 mg hair conditioner. Air was passed through the flask and fed into the OFR.

Section S2: D_5 gas sampling quality control results

Sufficient elution volume was tested by collecting a second cartridge elution of 1.5 mL for the sample with the highest anticipated concentration. Mass in the second elution was negligible compared to the primary elution (2.5% and 1.9% in duplicate testing). A cartridge breakthrough test was performed under the highest anticipated concentration sampling conditions, where a backup cartridge was connected behind the primary cartridge in the sampling setup. The backup cartridge was eluted into a separate GC vial and analyzed. Mass on the backup cartridge was negligible compared to the primary cartridge (0.6% in both duplicates).

Quality Control was assessed through a blank spike test; duplicates; and field, instrument, and method blanks. In the blank spike test, cleaned sample cartridges were spiked with D_5 and eluted with hexane to determine D_5 recovery from cartridges. Recoveries were 96% and 97% in duplicate testing. Duplicate samples and blanks were collected and analyzed. Relative percent difference ranged from 1 to 7% in the method blank duplicates, 1 to 13% in the field blank duplicates, 1 to 3% for the upstream sample duplicates, and 1 to 21% for the downstream sample duplicates. Contamination during sample deployment and handling in the field was monitored by analyzing field blanks. Mass on the field blanks ranged from 9 to 56 ng per blank. Contamination from glassware, cartridges, and solvents was monitored by analyzing method blanks which consisted of cleaned sample cartridges stored in a clean media fridge until analysis. Two method blanks per yield test were run through the extraction process in parallel with the samples. Mass on the method blanks ranged from 10 to 67 ng. Samples were not blank corrected.

Section S3: D_5 gas sampling details

Table S2: GC and MS parameters for D_5 gas concentration quantification.

GC parameters	Injector	3 washes in DCM, 3 washes in hexane pre- and post-injection
		3 sample pumps
		Fast plunger speed
		Injection volume 2 µL with a 10 µL syringe
	Oven Program	Initial temperature 60 ºC, hold 2 min
		Rate 20 ºC/min to final temp 250 ºC, hold 5 min
		Total run time 16.5 min
		Flow 0.8 mL/min
	Inlet	Helium carrier gas
		Splitless mode
		Temperature 200 ºC
		Pressure 5.3 psi
		Purge flow 50 mL/min, purge time 1 min, flow 53.6 mL/min
		Gas saver 20 mL/min, saver time 2 min
		3 min solvent delay
	Transfer line	Temperature 280 ºC
	Post run	5 min at 60 ºC
MS parameters	temperatures	MS source 250 ºC, MS quad 150 ºC
SIM mode	Ions monitored	355 (D_5) and 258 (PCB 30)

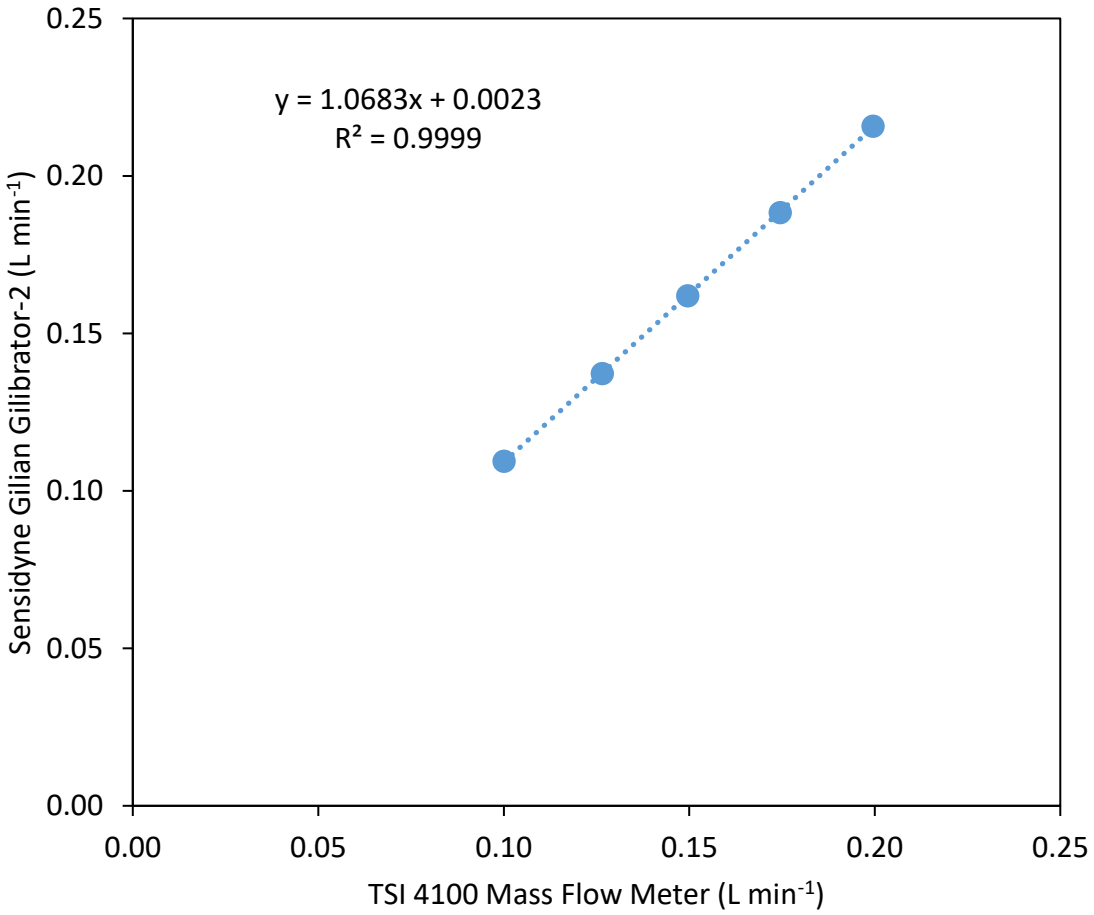

Figure S3: Calibration fit used to convert measured mass flow (TSI 4100) to volumetric flow for D_5 gas sampling. The volumetric flow was determined using a Sensidyne Gillian Gilibrator-2.

Table S3: D_5 gas sampling details. Samples with D_5 measured upstream of the OFR chamber are labeled "US", concentrations measured downstream of the reactor are labeled "DS". The label "P" and "B" refer to primary and backup cartridges, respectively. The reported flowrates are the calibrated volumetric flow rates.

Test	Sample	Sampling Time (min)	Average Flowrate (L min^{-1})	Total Volume (L)	Measured D_5 (ng)	D_5 Concentration (µg m^{-3})
Breakthrough	US1P	20.2	0.161	3.24	2619.3	808.2
Breakthrough	US2P	20.6	0.159	3.27	2645.3	809.3
Breakthrough	US1B	20.2	0.161	3.24	15.3	4.7
Breakthrough	US2B	20.6	0.159	3.27	14.8	4.5
Chamber Test	US1	20.0	0.162	3.24	1421.3	439.1
Chamber Test	US2	20.0	0.162	3.23	1387.5	429.3
Chamber Test	DS1	20.0	0.163	3.25	1400.7	430.4
Chamber Test	DS2	20.0	0.163	3.25	1387.0	426.4
Yield 1	US1	20.0	0.162	3.25	2399.5	739.2
Yield 1	US2	20.0	0.163	3.26	2413.4	740.7
Yield 1	DS1	20.0	0.167	3.33	54.9	16.5
Yield 1	DS2	20.0	0.166	3.32	44.4	13.4
Yield 2	US1	20.0	0.164	3.28	1210.2	369.5
Yield 2	US2	20.0	0.164	3.28	1243.7	378.8
Yield 2	DS1	20.0	0.164	3.28	59.3	18.1
Yield 2	DS2	20.0	0.164	3.28	58.7	17.9
Yield 3	US1	20.0	0.165	3.30	1628.4	493.8
Yield 3	US2	20.0	0.164	3.28	1679.4	511.3
Yield 3	DS1	20.0	0.162	3.24	68.0	21.0
Yield 3	DS2	20.0	0.161	3.23	78.2	24.2
Yield 4	US1	20.2	0.163	3.29	1246.3	378.9
Yield 4	US2	20.2	0.161	3.26	1207.6	370.8
Yield 4	DS1	20.2	0.159	3.21	55.9	17.4
Yield 4	DS2	20.1	0.158	3.16	48.6	15.4
Yield 5	US1	20.0	0.162	3.25	929.1	286.1
Yield 5	US2	20.0	0.162	3.25	954.9	294.1
Yield 5	DS1	20.0	0.166	3.31	32.5	9.8
Yield 5	DS2	20.0	0.164	3.28	30.7	9.4

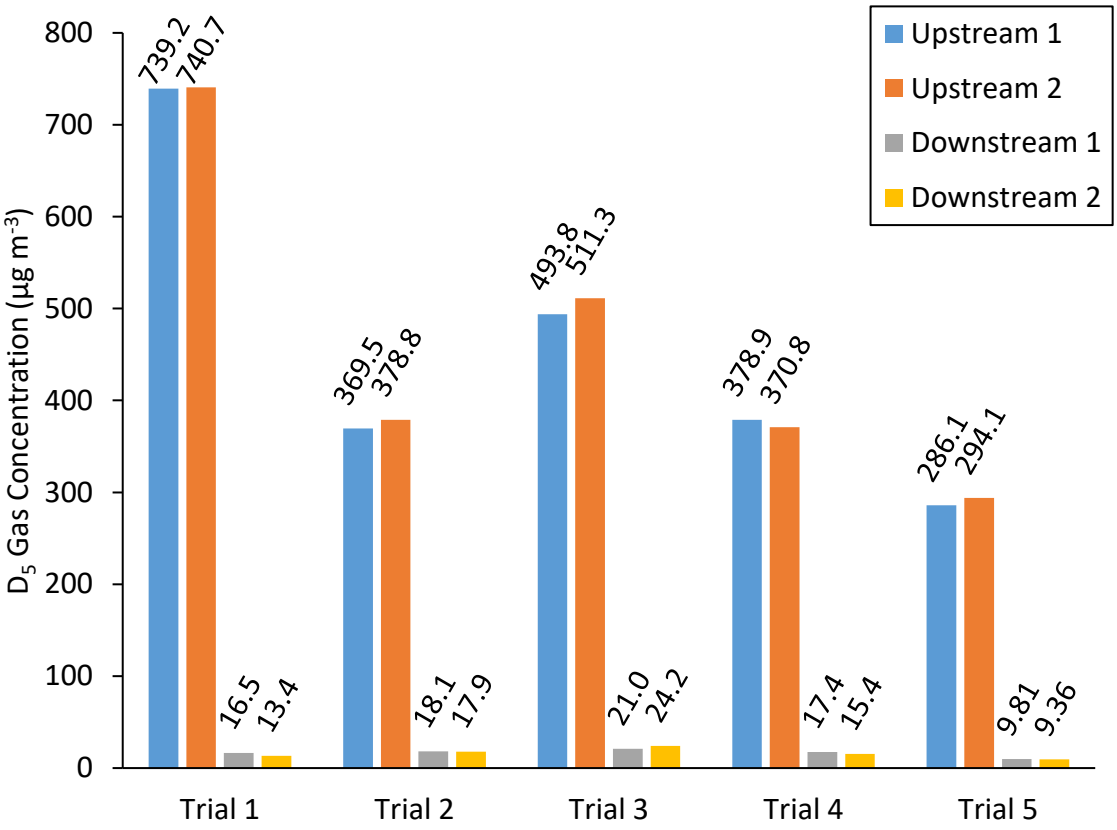

Figure S4: D_5 gas concentrations (µg m^{-3}) were quantified upstream and downstream of the OFR using SPE cartridges. Upstream 1 and 2, and downstream 1 and 2 refer to the duplicate trials.

Section S4: Particle loss correction

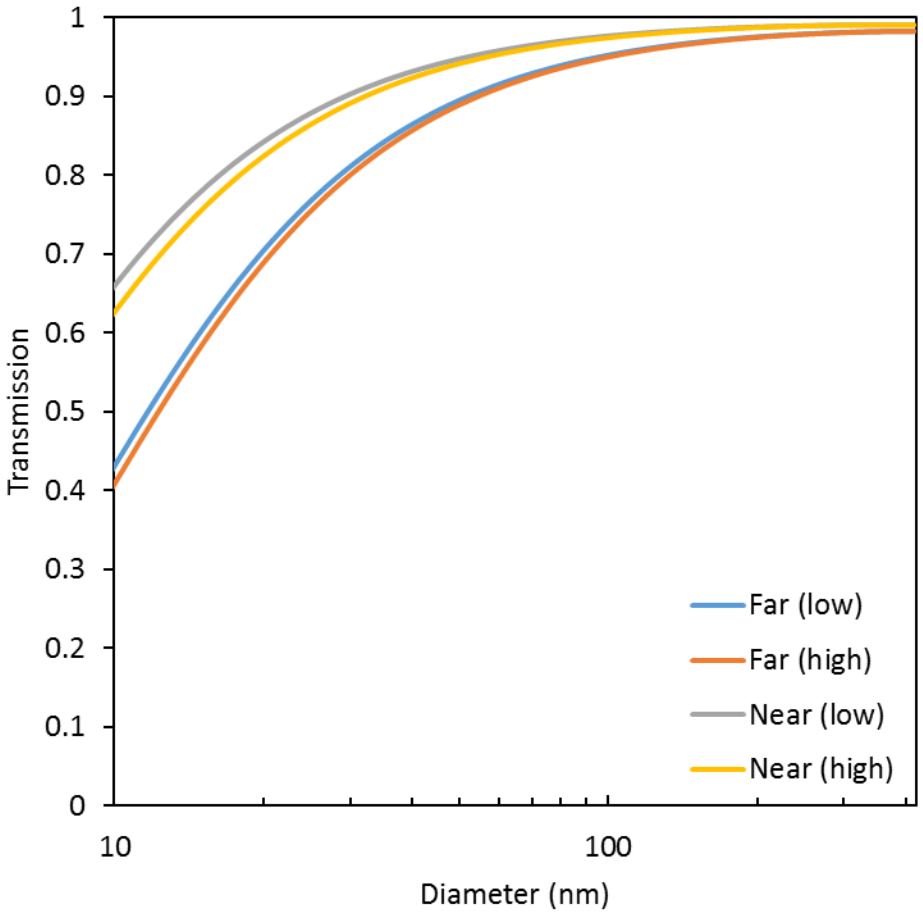

Figure S5: Modeled particle transmission for configurations with D_5 gas sampling. Far and near refer to SMPS placement relative to the OFR. Low and high refers to the incoming total flow of 3.5 L min^{-1} or 5 L min^{-1}, respectively.

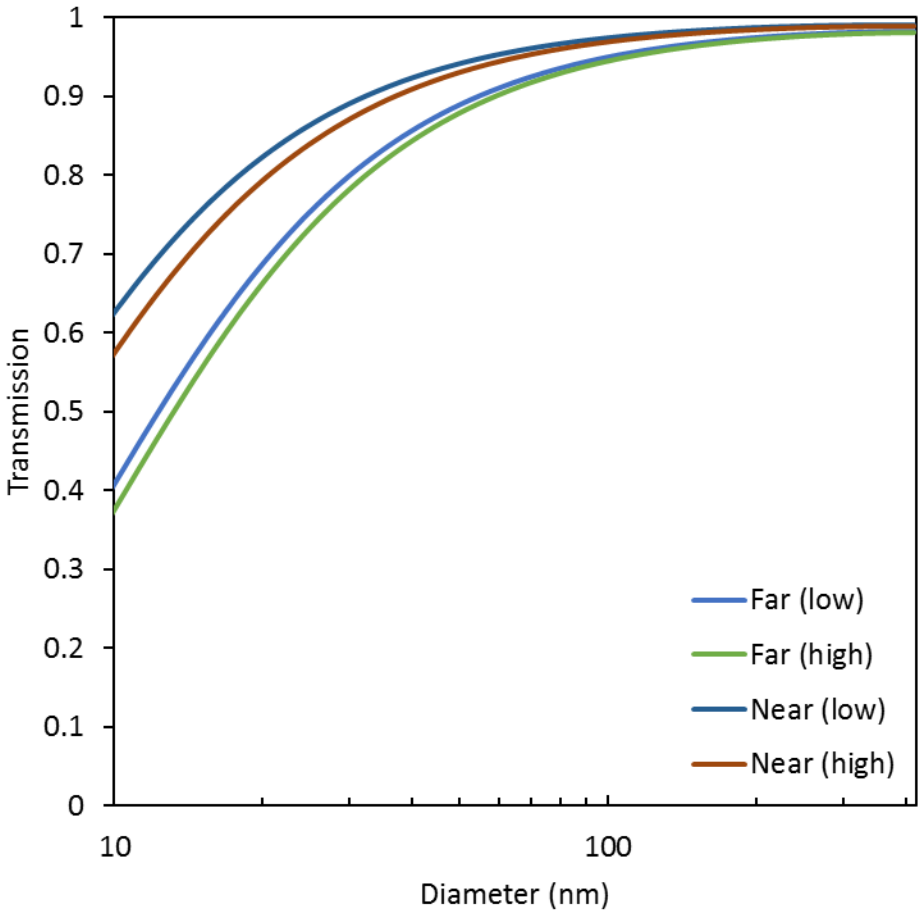

Figure S6: Modeled particle transmission for configurations with SO_2 gas sampling. Far and near refer to SMPS placement relative to the OFR. Low and high refers to the incoming total flow of 3.5 L min^{-1} or 5 L min^{-1}, respectively.

Table S4: List of corresponding SMPS placement and flow conditions for particle transmission correction.

Yield Test	SMPS Placement	Flow
1	Far	Low
2	Near	Low
3	Far	High
4	Far	Low
5	Near	High

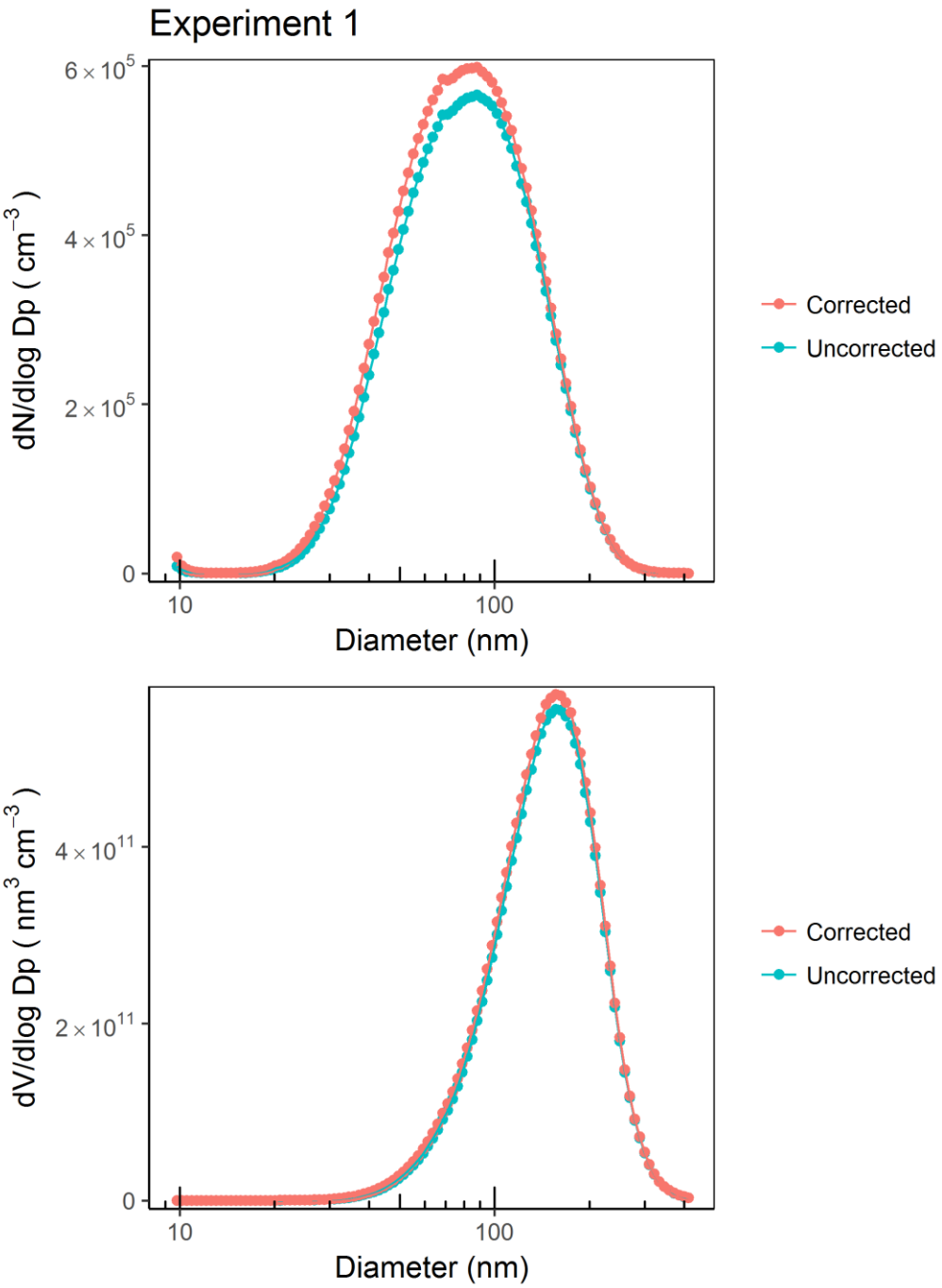

Figure S7: SMPS measured average number and volume D_5 oxidation aerosol size distributions for the yield experiment period. Corrected distributions are corrected for modeled particle losses in the denuders and tubing.

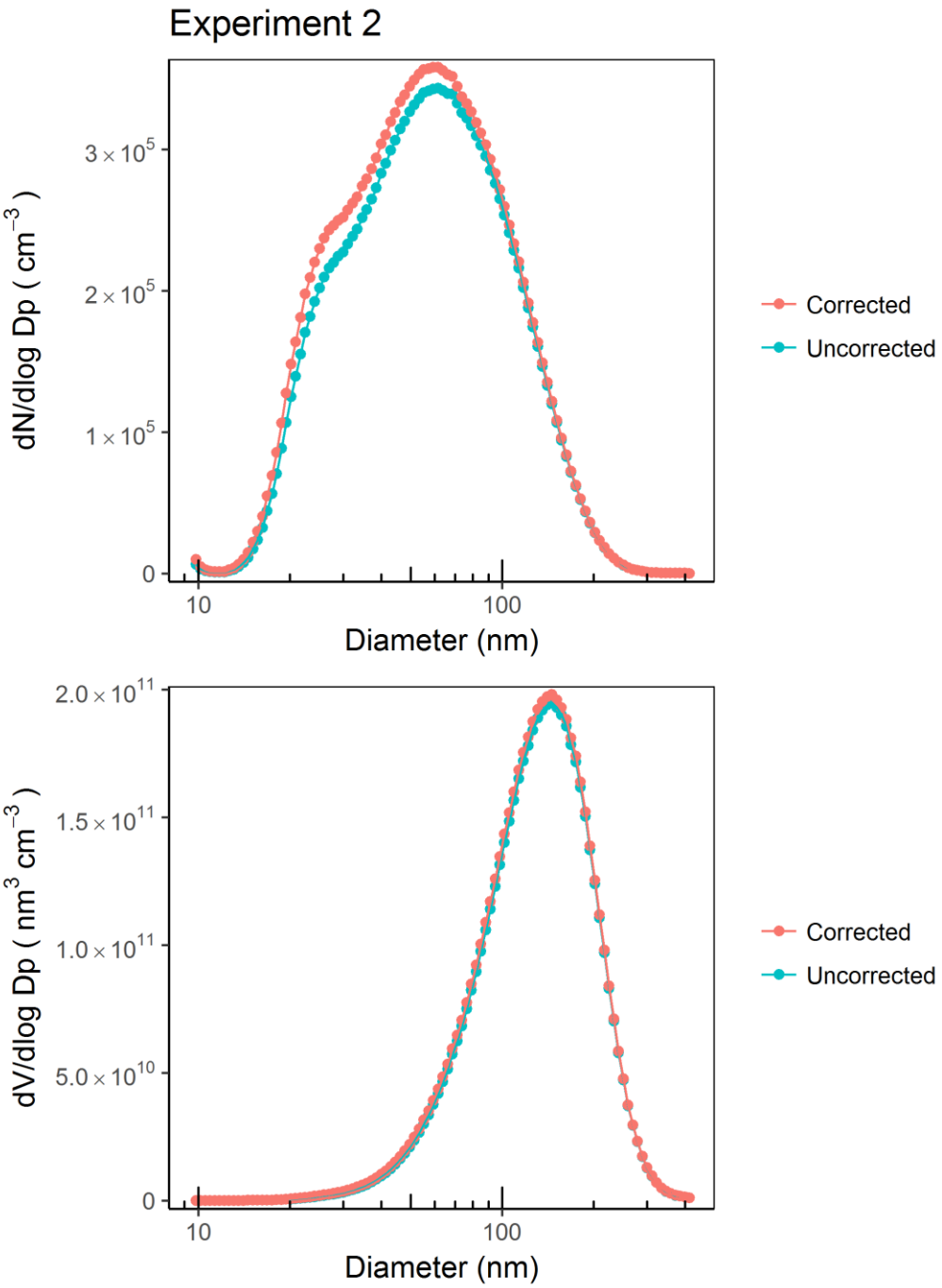

Figure S7: Continued

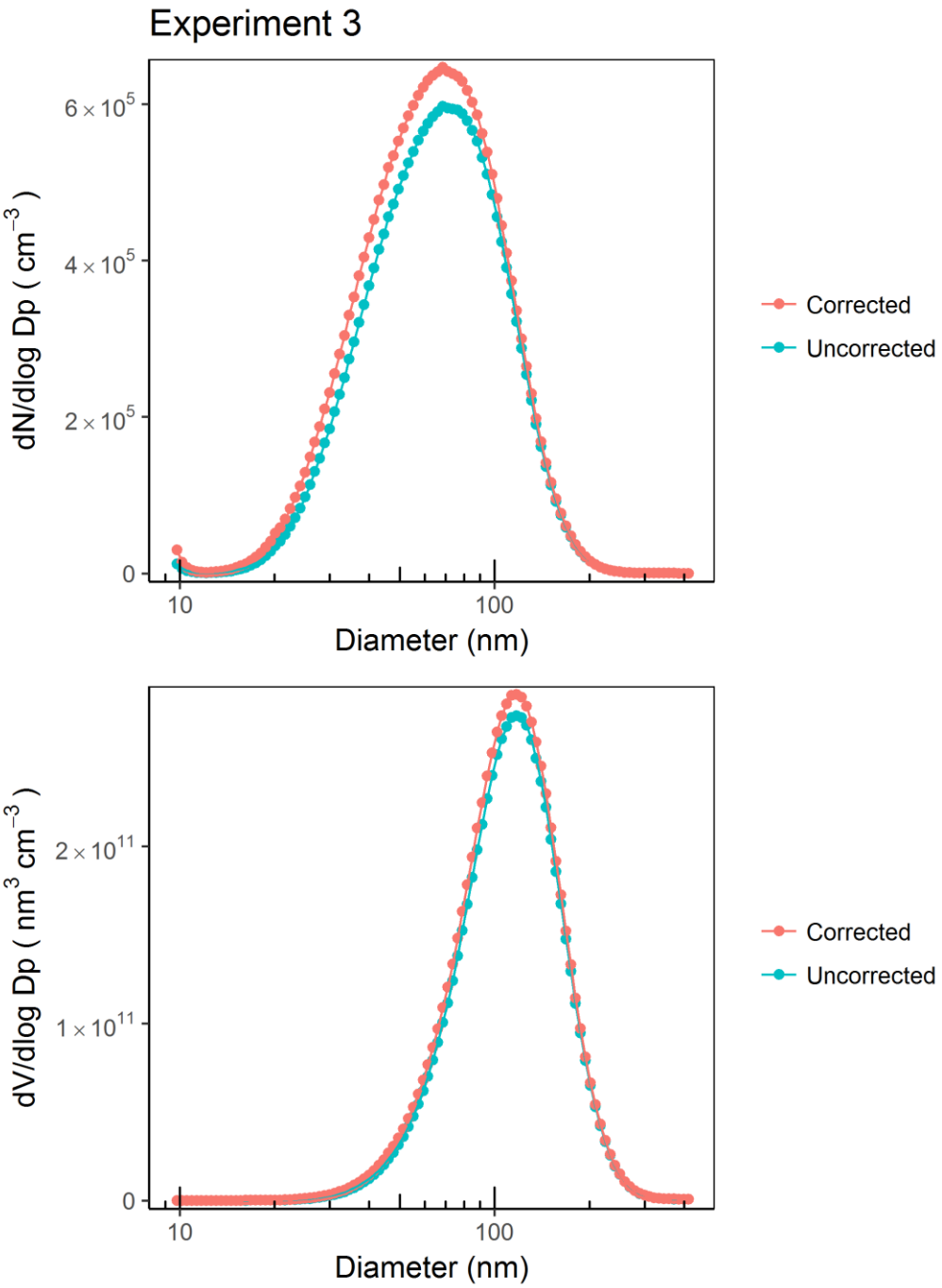

Figure S7: Continued

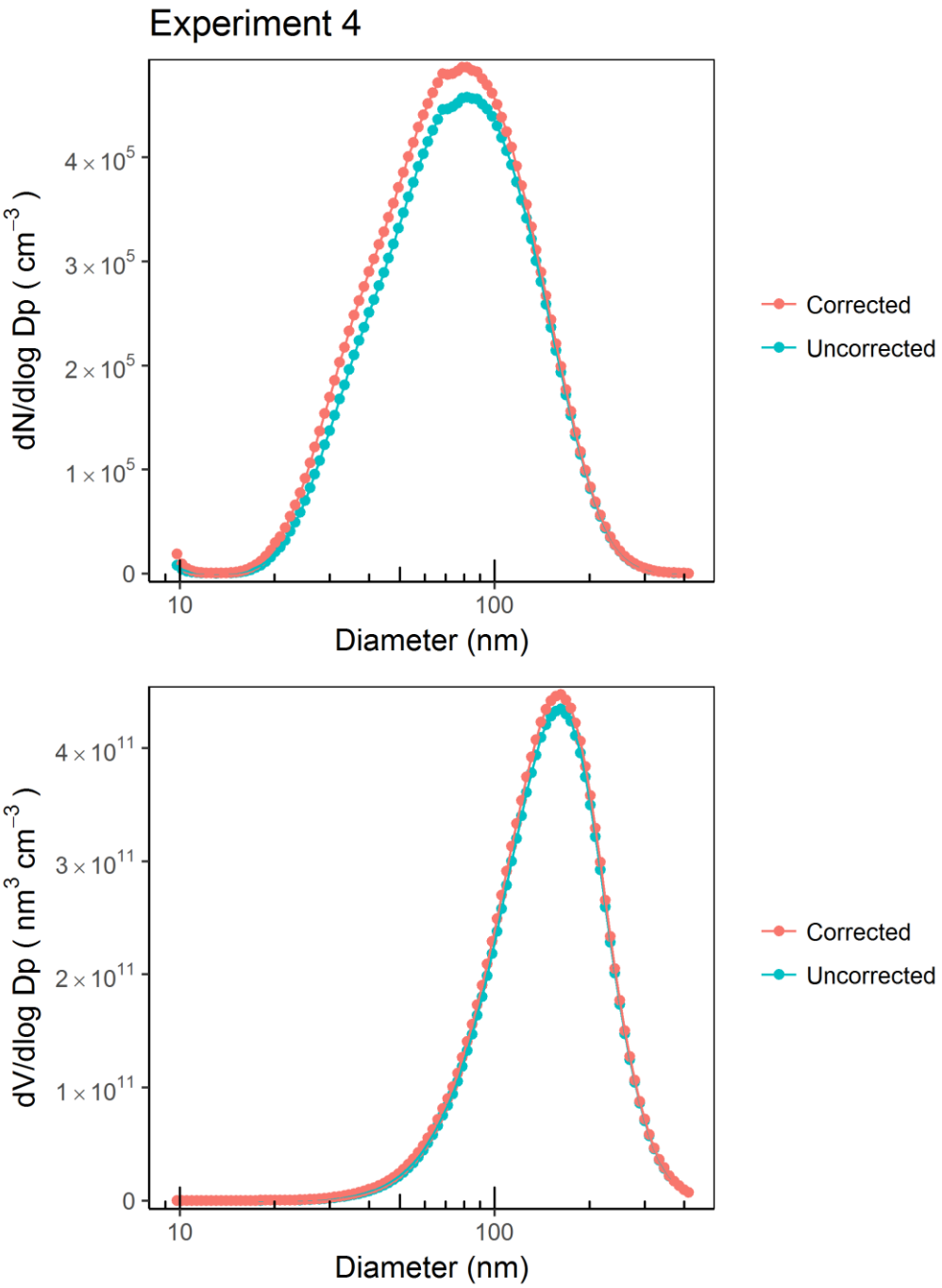

Figure S7: Continued

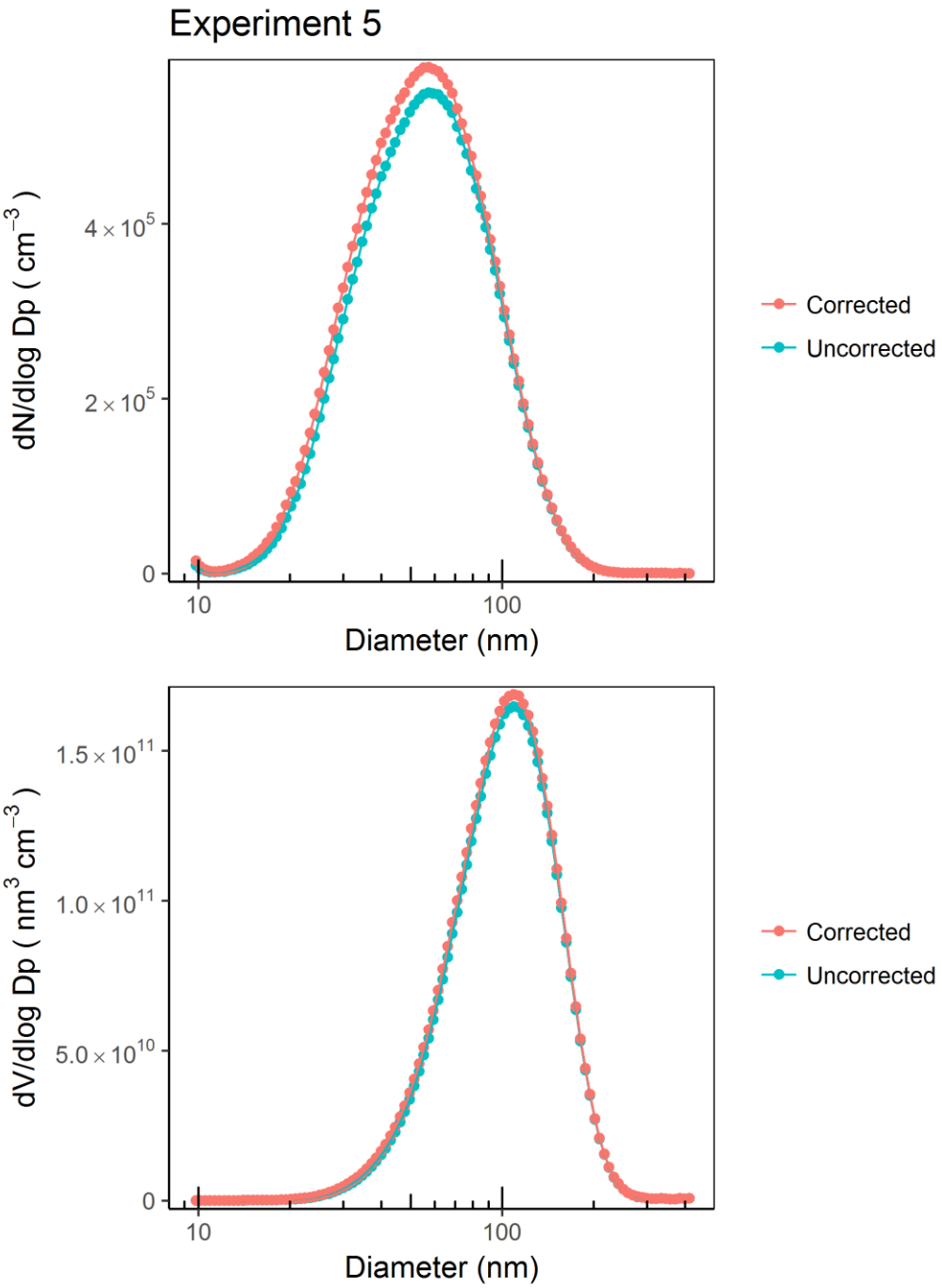

Figure S7: Continued

Section S5: Yield sensitivity

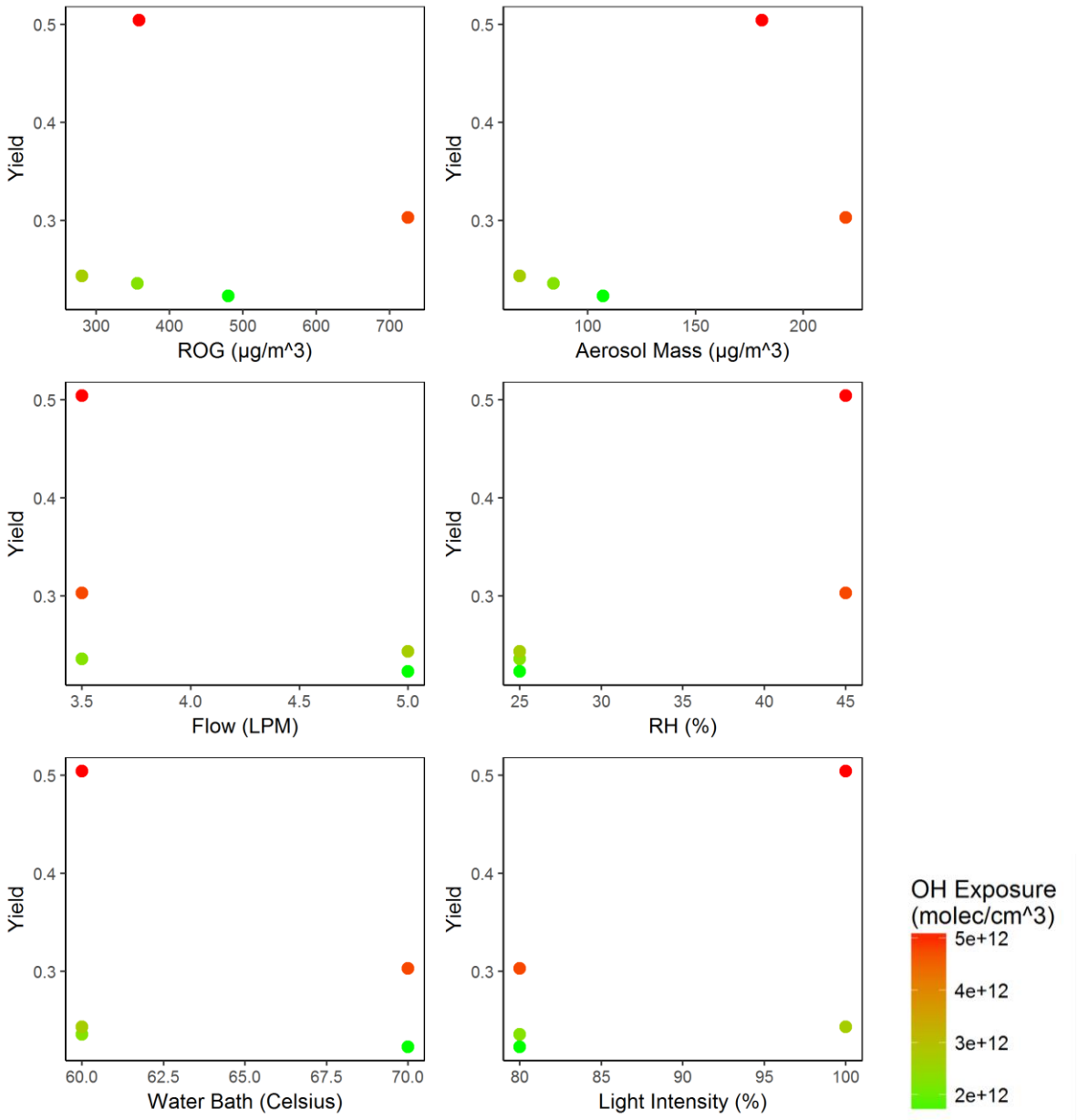

Figure S8: Measured D_5 oxidation aerosol yield as a function of system parameters. Data points are color coded according to OH exposure.

Section S6: Condensational sink input

Table S5: Calculated condensational sink (CS) calculations used for LVOC modeling (Sect. 3.2.1). CS was calculated according to Palm et al. (2016) which recommends the average of the incoming and output OFR CS. For the yield experiments, the output D_5 oxidation aerosol number concentration was averaged with 0 particle incoming air.

Experiment	Incoming Aerosol (cm^{-3})	Output Aerosol (cm^{-3})	CS (m^{-2})	CS rate (s^{-1})
Yield 1	0	3.47E+05	6619	0.3860
Yield 2	0	2.57E+05	3427	0.1998
Yield 3	0	3.58E+05	5173	0.3017
Yield 4	0	3.07E+05	5471	0.3190
Yield 5	0	3.31E+05	4035	0.2353

Section S7: Hygroscopicity

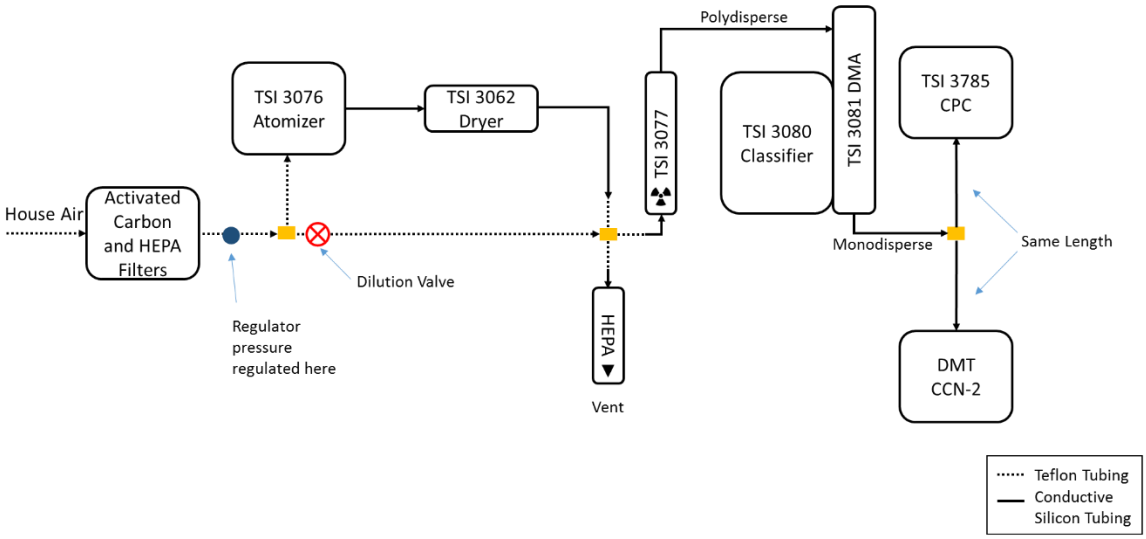

Figure S9: Ammoniums sulfate aerosol CCN testing flow diagram.

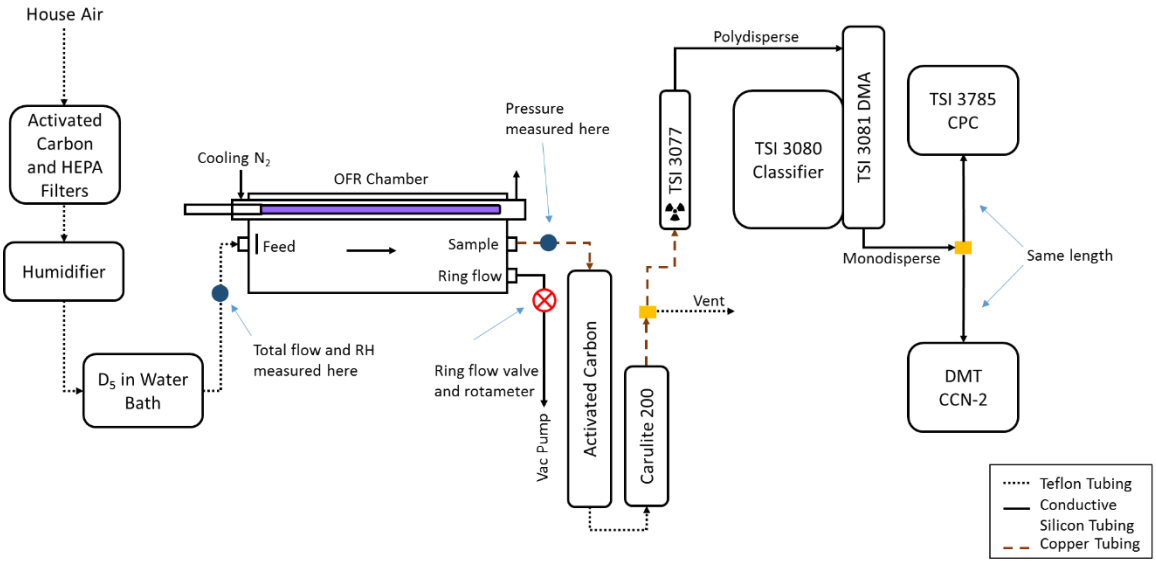

Figure S10: D_5 oxidation aerosol CCN testing flow diagram.

Two issues complicated CCN counter data analysis. First, temperature and flow spikes were observed that were caused by intermittent faults in a sample temperature sensor. This sensor was part of the instrument feedback control loop used to maintain the column thermal gradient, and accordingly these sensor faults upset the column thermal gradient and required some time to settle. Second, for some of the higher ΔT set points, the temperatures were not able to reach the set points but were stable. To correct for these issues, scripts were developed to automatically classify data into stable (used in data analysis) and unstable (excluded) periods. Data were initially binned to 30 s intervals (raw CCN data was at 1 s, CPC data was at 5 s). For each 30 s period, temperature, flow, and pressure stability were calculated and compared to thresholds as described below; periods were then flagged as stable or unstable.

Four temperature tests were used: (i) ΔT varied by no more than 0.16 K from the previous 10 s moving average; (ii) T1 (column low temperature) varied by no more than 0.20 K from the previous 10 s moving average; (iii) T3 (column high temperature) varied by no more than 0.20 K from the previous 10 s moving average; and (iv) that the 1 s values of ΔT varied by no more than 0.37 K during the 30 s period. Pressure and flow were checked individually to make sure the relative percent difference between the current value and the 10 s moving average was lower than 4.5%. These data exclusion thresholds were selected by visual inspection of the data, but final data processing was automated. Failure of a single test in any 30 second period led to exclusion from analysis. For periods compliant with these tests (70%), average CCN and CPC concentration were calculated along with the average ΔT.

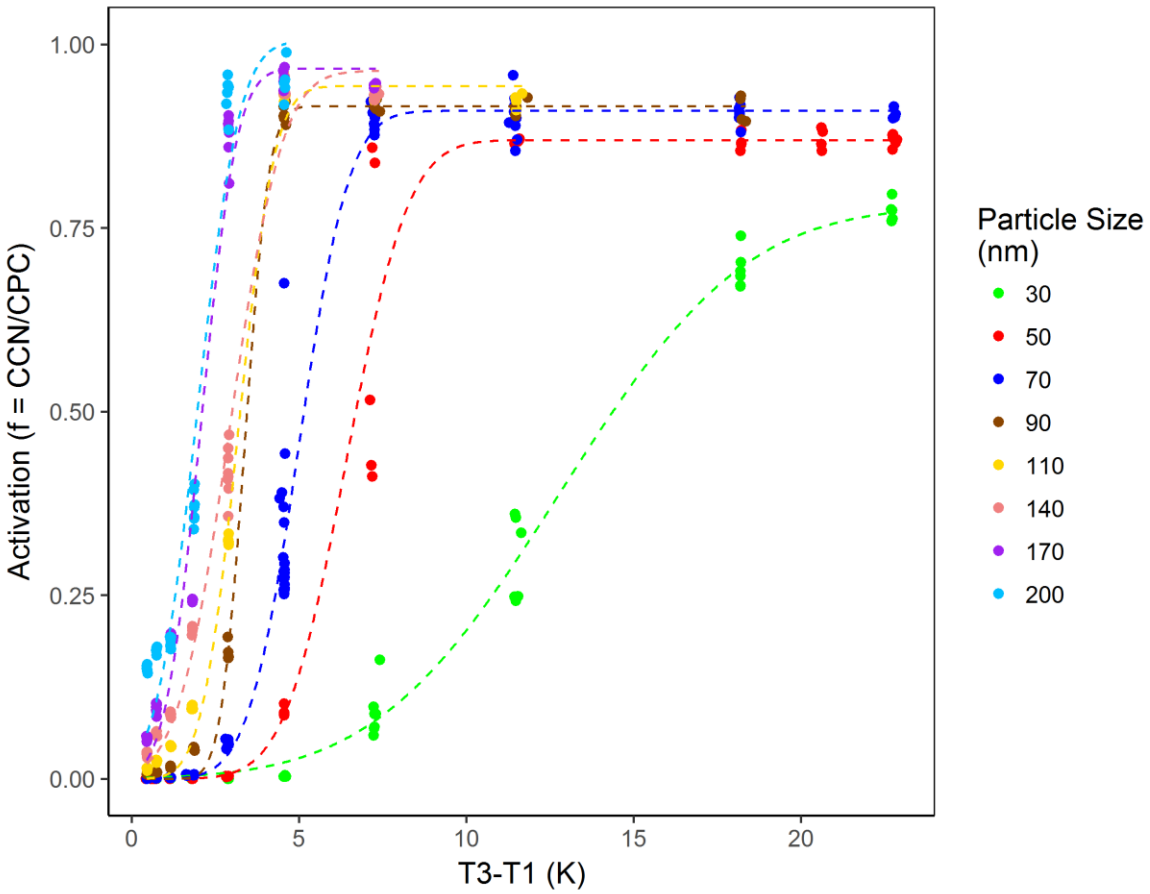

Figure S11: Uncorrected ammonium sulfate aerosol CCN activation curve used for calibration of the CCN counter supersaturation. Each point represents an average 30 s CCN/CPC measurement.

The AP3 Kohler model was used to relate ammonium sulfate particle diameter to critical supersaturation. The AP3 Kohler model is detailed in Rose et al. (2008). The critical supersaturation is found by writing all equations in terms of the unknown solute mass fraction (x_s) and finding the peak of the resultant Kohler curve.

AP3 Model Parameterization:

1. $\mu_s = \frac{x_s}{M_s(1-x_s)}$
2. a_w is found using a lookup table from the AIM inorganic model of a_w vs μ_s data. The AIM data was run using the web interface for 299.8 K (Clegg et al., 1998; Clegg et al.). The temperature 299.8 K is the average T1 column temperature of the experiments. The T1 temperature was suggested by Rose et al. (2008) since activation is assumed to occur in the first half of the column and the T1 temperature represents the lower bound for the effective column temperature. Linear interpolation was used for the resulting lookup table.
3. $\rho_w = \frac{A_0+A_1*t+A_2*t^2+A_3*t^3+A_4*t^4+A_5*t^5}{1+B_t}$

   t = T – 273.15 K

   Coefficients are found in Rose et al. (2008) Table A.4
4. $\rho_{sol} = \rho_w + \left[[5.92x10^{-3} * (100 * x_s)^1] + [-5.036x10^{-6} * (100 * x_s)^2] + [1.024x10^{-8} * (100 * x_s)^3]\right] * 1000$
5. $g_s = \left(\frac{\rho_s}{x_s*\rho_{sol}}\right)^{1/3}$

   ρ_s = 1770 kg m^{-3} for $(NH_4)_2SO_4$
6. $\sigma_w = 0.0761 - 1.55x10^{-4} * (T - 273\ K)$
7. $\sigma_{sol} = \sigma_w + (2.17x10^{-3} * c_s)$
8. $c_s = \frac{x_s*\rho_{sol}}{M_s*1000}$
9. $s = a_w e^{\left(\frac{4*\sigma_{sol}*M_w}{\rho_w*R*T*g_s*D_s}\right)}$

Defined variables:

μ_s = molality of solute (mol kg^{-1})
x_s = solute mass fraction
M_s = molar mass of solute (0.1321395 kg mol^{-1})
a_w = activity of water
ρ_{sol} = density of solution (kg m^{-3})
ρ_w = density of pure water (kg m^{-3})
g_s = particle growth factor
σ_{sol} = surface tension of solution (N m^{-1})
σ_w = surface tension of pure water (N m^{-1})
c_s = molarity of solute (mol L^{-1})
s = water vapor saturation ratio
M_w = molar mass of water (0.0180153 kg mol^{-1})
R = gas constant (N m k^{-1} mol^{-1})
D_s = dry particle diameter (m)

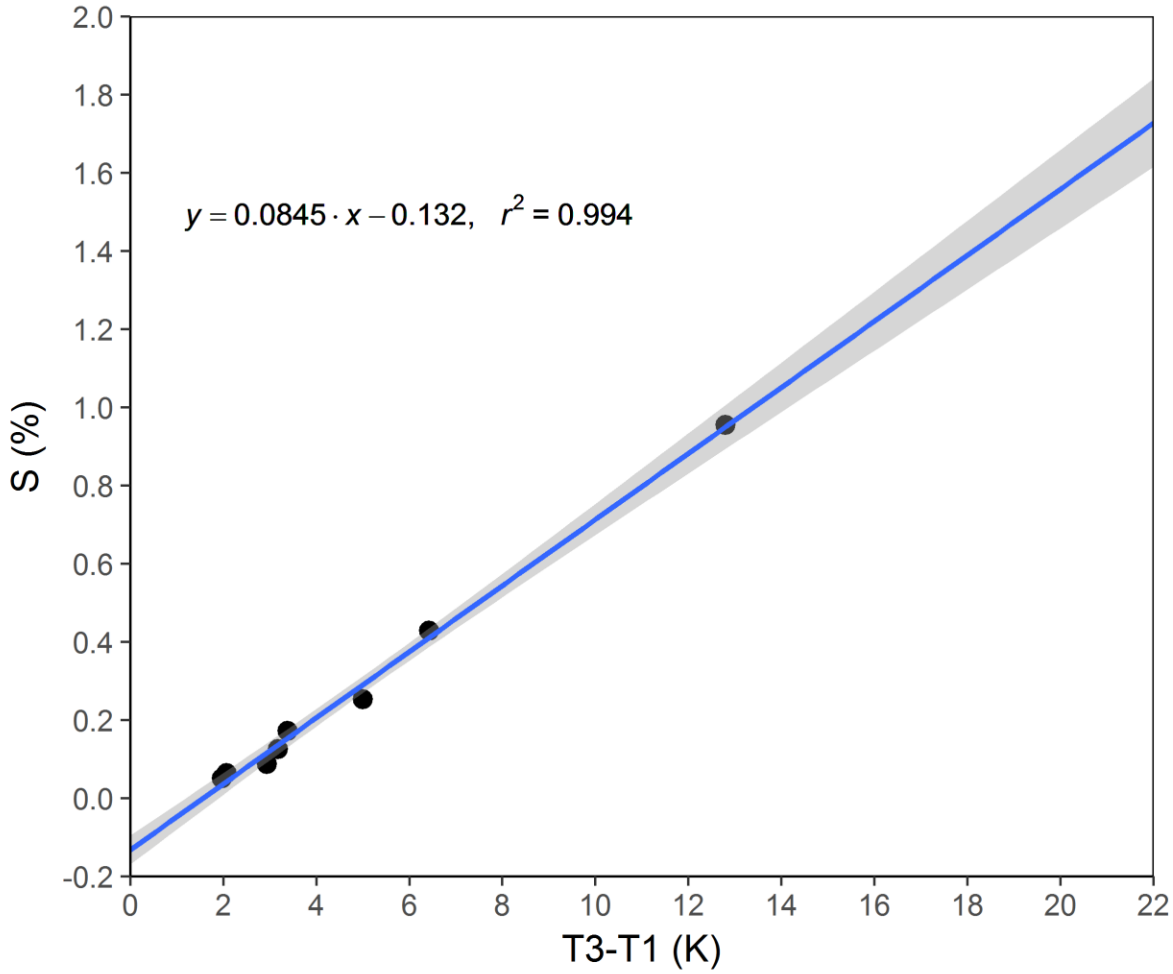

Figure S12: Supersaturation correlation to CCN counter ΔT based on ammonium sulfate aerosol calibration. Supersaturation was calculated using the AP3 Kohler model detailed in Rose et al. (2008). The shaded region represents the 95% confidence interval.

Table S6: Calculated size resolved kappa values for ammonium sulfate and D_5 oxidation aerosols.

Diameter (nm)	$(NH_4)_2SO_4$ (polynomial fit)	$(NH_4)_2SO_4$ (linear fit; 95% CI)	o-D_5 κ_a (linear fit; 95% CI)	o-D_5 κ_t (linear fit; 95% CI)
30	0.55	0.56 (0.49 - 0.63)	-	-
50	0.62	0.64 (0.57 - 0.72)	-	-
70	0.52	0.47 (0.40 - 0.54)	0.016 (0.014 - 0.020)	0.0056 (0.0042 - 0.0073)
90	0.97	0.78 (0.59 - 1.09)	0.010 (0.0084 - 0.012)	0.0056 (0.0044 - 0.0071)
110	0.66	0.54 (0.39 - 0.80)	0.012 (0.0099 - 0.014)	0.0060 (0.0049 - 0.0074)
140	0.42	0.36 (0.25 - 0.58)	0.0093 (0.0080 - 0.011)	0.0079 (0.0067 - 0.0093)
170	0.76	1.49 (0.55 - 11.4)	0.010 (0.0085 - 0.011)	0.0078 (0.0067 - 0.0091)
200	0.55	1.45 (0.44 - 43.4)	0.0068 (0.0058 - 0.0079)	0.0063 (0.0054 - 0.0073)
Average	0.63	0.79 (0.46 - 7.40)	0.011 (0.0091 - 0.013)	0.0065 (0.0054 - 0.0079)

Using a third order polynomial fit rather than the linear fit results in improved correlation for low supersaturations and a resulting average ammonium sulfate kappa of 0.63 which is in close agreement with the previously reported value of 0.61 (Petters and Kreidenweis, 2007). We use the linear fit however for the cVMS data due to improved performance at high supersaturations.

Section S8: Volatility

Table S7: Summary of V-TDMA analyzed results. Values represent the average of all trials for the selected particle size and temperature. D_p Bypass (all temps) is the average bypass particle size for all temperature settings of a particular particle size.

T Set (°C)	D_p Set (nm)	T (°C)	D_p Bypass (nm)	D_p Heated (nm)	D_p Bypass (all temps) (nm)	Bypass Number (cm^{-3})	Heated Number (cm^{-3})	Bypass Mass ($\mu g\ m^{-3}$)	Heated Mass ($\mu g\ m^{-3}$)	Heated Trials	Bypass Trials	Diameter Change (%)	Number Change (%)
50	10	50.1	12.76	11.24	12.38	922	1288	0.00130	0.00121	2	2	-9.19	39.7
80	10	80.2	12.59	9.056	12.38	1044	556	0.00132	0.00196	4	2	-26.9	-46.8
110	10	110.4	14.71	10.96	12.38	1703	628	0.00291	0.000960	4	2	-11.5	-63.1
150	10	149.6	10.45	11.36	12.38	1753	544	0.00218	0.000656	3	3	-8.23	-69.0
190	10	191.4	-	9.040	12.38	-	119	-	0.000139	2	0	-27.0	-
50	20	49.8	20.75	20.45	20.68	37848	40177	0.169	0.175	3	1	-1.10	6.15
80	20	80.0	20.64	20.30	20.68	34577	36096	0.153	0.150	4	2	-1.81	4.39
110	20	109.8	20.68	20.18	20.68	35122	35217	0.156	0.141	4	2	-2.39	0.27
150	20	150.9	20.64	19.92	20.68	37235	30917	0.166	0.113	3	2	-3.68	-17.0
190	20	189.4	20.75	19.79	20.68	39831	26877	0.176	0.0911	2	1	-4.29	-32.5
50	30	50.0	30.14	30.05	30.19	70981	81449	1.00	1.14	2	1	-0.47	14.7
80	30	80.3	30.18	29.87	30.19	75440	78321	1.07	1.06	4	2	-1.07	3.82
110	30	110.5	30.19	29.52	30.19	72643	70515	1.02	0.911	4	2	-2.25	-2.93
150	30	149.9	30.19	29.18	30.19	74929	68995	1.06	0.840	4	2	-3.37	-7.92
190	30	189.8	30.30	28.89	30.19	69580	61425	0.994	0.686	2	1	-4.32	-11.7
50	50	50.0	49.85	49.63	49.89	70528	69382	4.54	4.42	2	1	-0.53	-1.63
80	50	80.1	49.96	49.37	49.89	67418	68649	4.36	4.20	4	2	-1.04	1.83
110	50	110.1	49.85	48.94	49.89	69197	66893	4.45	3.96	4	2	-1.91	-3.33
150	50	150.2	49.75	48.84	49.89	63422	65996	4.06	3.72	4	2	-2.10	4.06
190	50	191.1	50.16	48.29	49.89	70161	60349	4.58	3.19	2	1	-3.21	-14.0
50	80	50.1	80.28	79.87	80.14	46485	48112	12.6	12.8	3	1	-0.34	3.50
80	80	80.3	80.08	79.44	80.14	47606	46148	12.9	12.0	4	2	-0.88	-3.06
110	80	110.0	80.16	79.09	80.14	45690	44591	12.4	11.4	4	2	-1.32	-2.41
150	80	150.7	80.07	78.34	80.14	44614	43540	12.0	10.6	3	2	-2.26	-2.41
190	80	189.1	80.25	77.79	80.14	42705	39579	11.5	9.38	2	1	-2.94	-7.32
50	110	50.2	110.2	109.7	110.1	24992	23295	17.7	16.2	3	12	-0.40	-6.79
80	110	80.1	110.1	109.3	110.1	23384	23653	16.5	16.3	4	2	-0.72	1.15
110	110	110.6	110.1	108.6	110.1	25163	22110	17.7	14.9	4	2	-1.39	-12.1
150	110	149.4	110.0	108.1	110.1	23160	22130	16.3	14.7	3	3	-1.83	-4.45
190	110	190.5	109.9	107.9	110.1	20968	19948	14.8	12.9	2	1	-2.00	-4.86

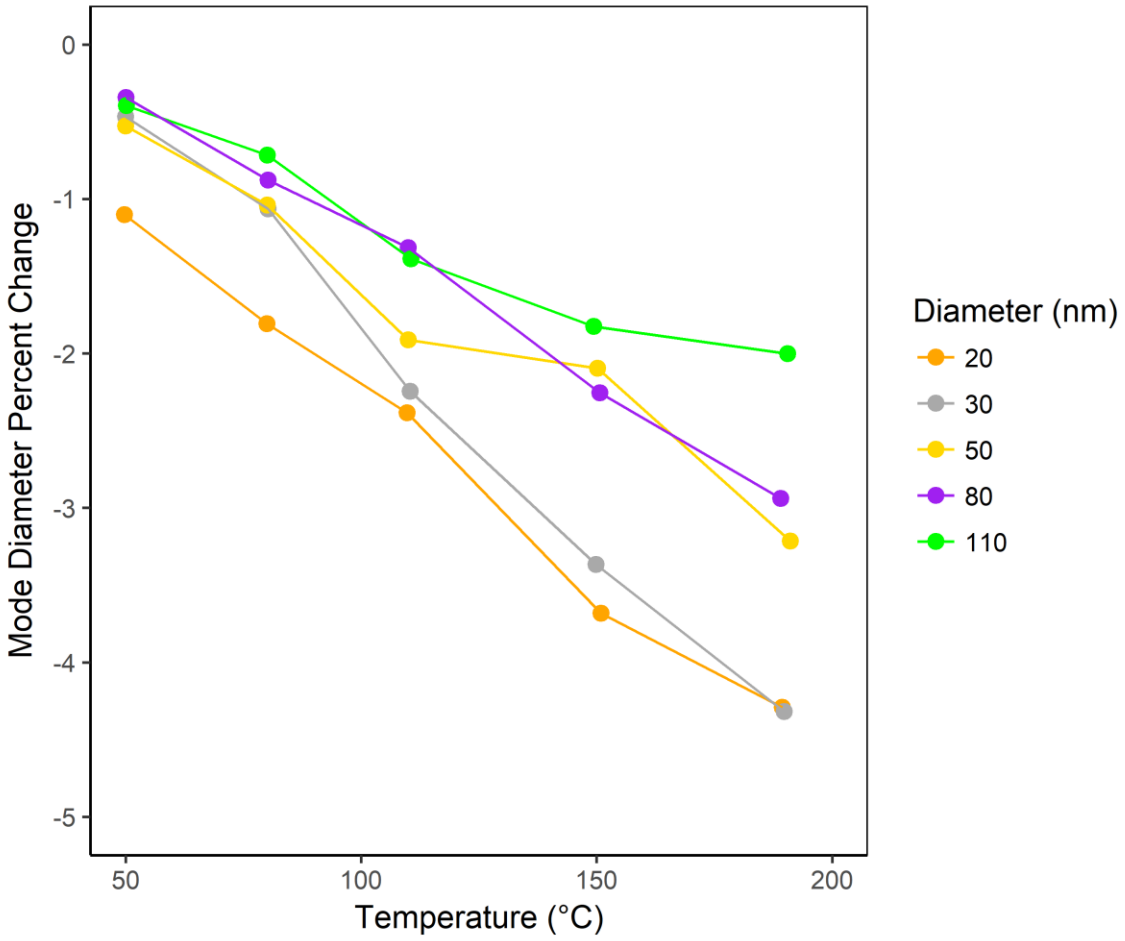

Figure S13: D_5 oxidation aerosol change in mode diameter after exposure to heated conditions in the V-TDMA experiments.

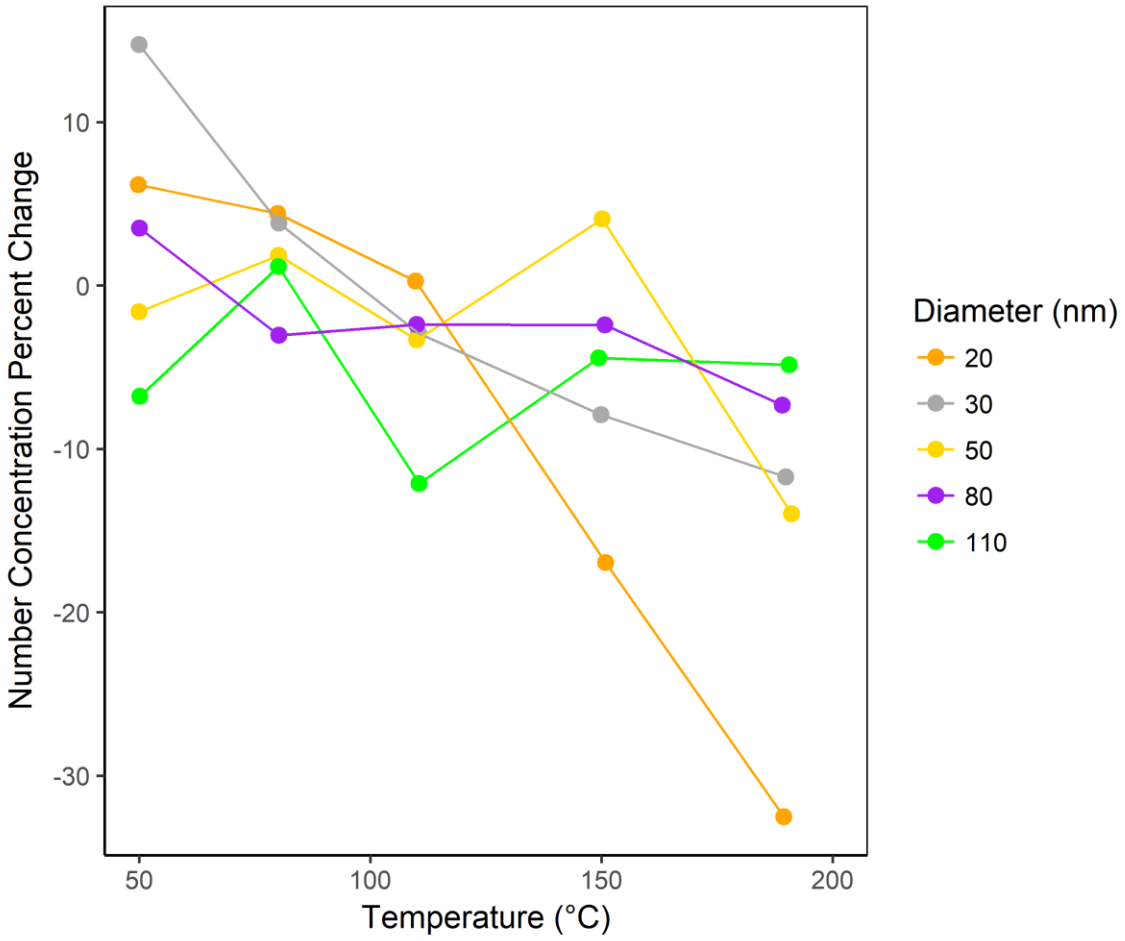

Figure S14: D_5 oxidation aerosol change in number concentration after exposure to heated conditions in the V-TDMA experiments.

References

Extended AIM Aerosol Thermodynamics Model: http://www.aim.env.uea.ac.uk/aim/aim.php, access: November 2017.

Clegg, S. L., Brimblecombe, P., and Wexler, A. S.: Thermodynamic Model of the System H+−NH4+−SO42-−NO3-−H2O at Tropospheric Temperatures, The Journal of Physical Chemistry A, 102, 2137-2154, doi:10.1021/jp973042r, 1998.

Palm, B. B., Campuzano-Jost, P., Ortega, A. M., Day, D. A., Kaser, L., Jud, W., Karl, T., Hansel, A., Hunter, J. F., Cross, E. S., Kroll, J. H., Peng, Z., Brune, W. H., and Jimenez, J. L.: In situ secondary organic aerosol formation from ambient pine forest air using an oxidation flow reactor, Atmos. Chem. Phys., 16, 2943-2970, doi:10.5194/acp-16-2943-2016, 2016.

Petters, M. D., and Kreidenweis, S. M.: A single parameter representation of hygroscopic growth and cloud condensation nucleus activity, Atmos. Chem. Phys., 7, 1961-1971, doi:10.5194/acp-7-1961-2007, 2007.

Rose, D., Gunthe, S. S., Mikhailov, E., Frank, G. P., Dusek, U., Andreae, M. O., and Pöschl, U.: Calibration and measurement uncertainties of a continuous-flow cloud condensation nuclei counter (DMT-CCNC): CCN activation of ammonium sulfate and sodium chloride aerosol particles in theory and experiment, Atmos. Chem. Phys., 8, 1153-1179, doi:10.5194/acp-8-1153-2008, 2008.